

THE EFFECT OF WAVE-PARTICLE INTERACTIONS ON LOW ENERGY CUTOFFS IN SOLAR FLARE ELECTRON SPECTRA

I. G. HANNAH¹, E. P. KONTAR¹, AND O. K. SIRENKO²

¹ Department of Physics and Astronomy, University of Glasgow, G12 8QQ, UK and

² Main Astronomical Observatory, Ukrainian Academy of Sciences, Ukraine

Draft version October 8, 2018

ABSTRACT

Solar flare hard X-ray spectra from RHESSI are normally interpreted in terms of purely collisional electron beam propagation, ignoring spatial evolution and collective effects. In this paper we present self-consistent numerical simulations of the spatial and temporal evolution of an electron beam subject to collisional transport and beam-driven Langmuir wave turbulence. These wave-particle interactions represent the background plasma's response to the electron beam propagating from the corona to chromosphere and occur on a far faster timescale than coulomb collisions. From these simulations we derive the mean electron flux spectrum, comparable to such spectra recovered from high resolution hard X-rays observations of solar flares with RHESSI. We find that a negative spectral index (i.e. a spectrum that increases with energy), or local minima when including the expected thermal spectral component at low energies, occurs in the standard thick-target model, when coulomb collisions are only considered. The inclusion of wave-particle interactions does not produce a local minimum, maintaining a positive spectral index. These simulations are a step towards a more complete treatment of electron transport in solar flares and suggest that a flat spectrum (spectral index of 0 to 1) down to thermal energies maybe a better approximation instead of a sharp cut-off in the injected electron spectrum.

Subject headings: Sun: flares - Sun: X-rays, gamma rays - Sun: activity -Sun: particle emission

1. INTRODUCTION

Hard X-ray emission has long been used as the prime diagnostic tool to study particle acceleration and energy release in solar flares. From these X-ray observations the mean electron flux spectrum (e.g. averaged over the X-ray emitting volume, see Brown et al. (2003) for details) can be determined either through forward fitting (Holman et al. 2003) or more advanced inversion techniques (Piana et al. 2003; Kontar et al. 2004; Brown et al. 2006). At higher energies, typically above 10-20 keV, the observed hard X-ray spectrum is considered to be due to an accelerated population of electrons being stopped by the dense chromosphere via Coulomb collisions (Brown 1971). The spectrum below 10-20 keV normally originates from thermal coronal sources with temperatures of 10s MK (e.g. Krucker & Lin 2008).

The Reuven Ramaty High Energy Solar Spectrometer (RHESSI) provides high resolution HXR spectra of solar flares (Lin et al. 2002), greatly improving on previous measurements (Johns & Lin 1992). This high energy resolution spectra has allowed, for the first time, to scrutinize the X-ray and electron spectra in search for a non-powerlaw features, revealing vital clues about electron acceleration and transport. In some RHESSI flares, the recovered mean electron flux spectrum demonstrates a local minima or *dip* between the non-thermal and the thermal components instead of a smooth transition (Piana et al. 2003; Holman et al. 2003; Kašparová et al. 2005; Sui et al. 2007; Kontar et al. 2008a). The presence of the dip, as a real physical feature of the electron spectra, has been questioned as in many cases it can be attributed to photospheric albedo, e.g. Compton back-scattered X-rays (Kašparová et al. 2005; Kontar et al. 2008a). However a few events have been found in which after isotropic albedo correction (Kontar et al. 2008a),

the X-ray spectrum is still relatively flat, so they could be fitted with a thick-target model single power-law spectrum with a low energy cutoff (Sui et al. 2007). In these flares a dip was not directly observed in the mean electron spectrum, but instead inferred from forward fitting a model with low energy cutoff to the X-ray spectrum. This model has a thermal component at low energies and at higher energies purely collisional thick-target model of a single power-law of accelerated electrons above a cutoff. In this thick-target scenario (Brown 1971; Holman 2003), the dip in the mean electron spectrum originates from a positive slope at low energies developing below the cut-off as the accelerated electrons propagate from a coronal acceleration site downwards to the chromosphere, having Coulomb collisions with the background plasma. If the dip is real it provides important insights into flare energetics since the energy in accelerated electrons is strongly dependent on the low energy cutoff.

For any reasonable X-ray producing flare, non-collisional beam-plasma interaction is much faster than that via Coulomb collisions (Zheleznyakov & Zaitsev 1970; Karlický 2009). Such processes are inferred to occur in downward propagating electron beams from radio observations of reverse slope drift burst in flares (e.g. Klein et al. 1997; Aschwanden & Benz 1997). Although generation and escape of electromagnetic radiation from Langmuir waves in a flaring plasma is not well understood. The role of wave-particle interactions in solar flares assuming stationary, time-independent injection of electrons have been considered analytically and numerically (Emslie & Smith 1984; Hamilton & Petrosian 1987; McClements 1987). Emslie & Smith (1984) have argued that the conditionally created distribution should be constantly being flattened by quasi-linear relaxation, while Hamilton & Petrosian (1987) and McClements (1987) suggest that although the wave-particle interactions have

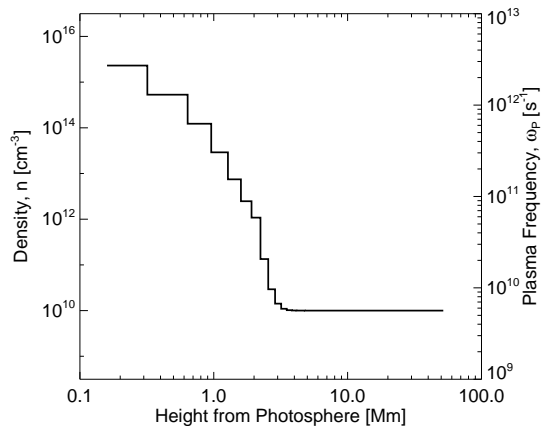


FIG. 1.— The background plasma density $n(x)$ as a function of the height above the photosphere. Also shown is the corresponding plasma frequency for each of these densities.

an important effect, the change of the electron spectra under stationary conditions should be minor. However, in a more realistic flare conditions the injection (acceleration) of electrons is likely to be highly intermittent (Tsiklauri & Haruki 2008) with a number of short duration pulses is often observed (Kiplinger et al. 1984; Fleishman et al. 1994; Aschwanden et al. 1998), so the time-dependent solution of particle transport equations accounting for wave-particle interactions should be considered. Additionally, the previous studies did not consider the spatial and temporal evolution of the beam from the coronal source down into chromosphere - a crucial aspect when considering the propagation of an electron beam in comparison to X-ray observations.

The quasi-linear relaxation process of Langmuir waves has been considered in higher velocity dimensions (other than the parallel component considered here) (e.g. Churaev & Agapov 1980) but it has only been recently that the 2D system has been fully numerically solved (Ziebell et al. 2008). Even then the evolution was considered in a spatially independent manner. In these studies it was found that the parallel component (1D) is the fastest processes and likely to dominate the electron transport.

In this letter we take a step towards a more complete treatment of electron transport in solar flares by including the spatial evolution of beam-driven Langmuir wave turbulence. We numerically study the system self-consistently, simulating the propagation of an electron beam from the coronal acceleration site down to the chromosphere, considering the truncated power-law spectrum frequently used for data interpretation (e.g. Holman 2003; Sui et al. 2007), to investigate the evolution of the mean electron flux spectrum below this cut-off. We demonstrate that the positive slope of the mean electron flux is not present, when the response of the background plasma via Langmuir waves to the propagating electron beam is taken into account. We also show that the injected electron spectrum flattens to a decreasing distribution due to collective interaction with plasma even for weak flares (e.g. Hannah et al. 2008a). Furthermore, we suggest that a flat spectrum (with spectral index 0 to 1) down to thermal energies maybe a better approximation as opposed to the sharp cut-off in the

injected electron spectrum.

2. PARTICLE TRANSPORT AND WAVE-PARTICLE INTERACTION

Following the standard model approach for interpreting solar flare hard X-ray spectra, we assume the electron flux spectrum of injected (flare accelerated) electrons is a power law, $F(E) \sim E^{-\delta}$, [electrons $\text{cm}^{-2} \text{s}^{-1} \text{keV}^{-1}$] down to some energy E_C , typically 10-20 keV. The initial 1D electron distribution function (accelerated electron population) subsequently is also a power-law in velocity $f(v) = F(E)/m$, above a low energy cutoff v_C with spectral index $\alpha = 2\delta$. For our simulations we consider such an initial electron distribution which is also spatially a gaussian of characteristic size d

$$f(v, x, t = 0) = n_0 \frac{(1 - \alpha)}{v_C} \left(\frac{v}{v_C} \right)^{-\alpha} \exp\left(-\frac{x^2}{d^2}\right) \quad (1)$$

normalised by the beam density n_0 .

To self-consistently follow the temporal and spatial evolution of an electron beam from a coronal acceleration site, including the response of the thermal background plasma in the form of Langmuir waves, we use the 1D equations of quasi-linear relaxation (Vedenov & Velikhov 1963; Drummond & Pines 1964; Ryutov 1969; Hamilton & Petrosian 1987; Kontar 2001a)

$$\frac{\partial f}{\partial t} + v \frac{\partial f}{\partial x} = \frac{4\pi^2 e^2}{m^2} \frac{\partial}{\partial v} \left(\frac{W}{v} \frac{\partial f}{\partial v} \right) + \gamma_{CF} \frac{\partial}{\partial v} \left(\frac{f}{v^2} \right) \quad (2)$$

$$\frac{\partial W}{\partial t} + \frac{3v_T^2}{v} \frac{\partial W}{\partial x} = \left(\frac{\pi\omega_p}{n} v^2 \frac{\partial f}{\partial v} - \gamma_{CW} - 2\gamma_L \right) W + Sf \quad (3)$$

where $f(v, x, t)$ is the electron distribution function [electrons $\text{cm}^{-4} \text{s}$], $W(v, x, t)$ is the spectral energy density [erg cm^{-2}], k is the wave number of a Langmuir wave, n is the background plasma density and $\omega_p^2 = 4\pi n e^2 / m$ is the local plasma frequency. The first component on the righthand side of equations (2) and (3) are the quasilinear terms that describes the resonant interaction between the electrons and Langmuir waves, $\omega_p = kv$. Also included are the Coulomb collision dampening rate for both the electrons $\gamma_{CF} = 4\pi e^4 n \ln \Lambda / m^2$ (Emslie 1978) and waves $\gamma_{CW} = \pi e^4 n \ln \Lambda / (m^2 v_T^3)$ (Melrose 1980). Where $\ln \Lambda = \ln(8 \times 10^6 n^{-1/2} T)$ is the Coulomb logarithm, T is the temperature of the background plasma and $v_T = \sqrt{k_B T / m}$ is the velocity of a thermal electron, k_B is the Boltzmann constant. Also included in equation (3) is the Landau dampening rate $\gamma_L = \sqrt{\pi} / 8 \omega_p (v/v_T)^3 \exp(-v^2/2v_T^2)$ (Lifshitz & Pitaevskii 1981) and the spontaneous emission $S = \omega_p^3 m v \ln(v/v_T) / (4\pi n)$ (Melrose 1980; Tsytovich & Terhaar 1995; Hamilton & Petrosian 1987).

In the simulations, we take $\alpha = 7$, or $\delta = 3.5$ from a cutoff of $v_C = 7.26 \times 10^9 \text{ cm s}^{-1}$, or $E_C = 15 \text{ keV}$, up to maximum of $v_0 = 2.4 \times 10^{10} \text{ cm s}^{-1}$. Our simulation extends in velocity space from $v = 7v_T = 2.73 \times 10^9 \text{ cm s}^{-1}$ (taking $T = 1 \text{ MK}$) to $v = 2.5 \times 10^{10} \text{ cm s}^{-1}$. The initial spatial scale of the beam is $d = 2 \times 10^8 \text{ cm}$ with

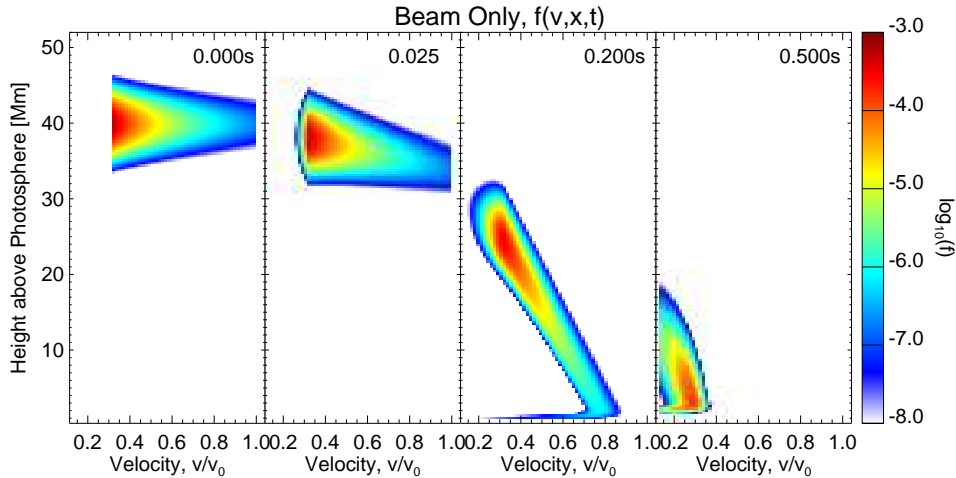


FIG. 2.— The evolution of the electron distribution $f(v, x, t)$ (with time increasing from left to right) for the simulation only following the progression of an electron beam subject to Coulomb collisions, i.e. the standard thick-target model (Brown 1971). (An animation of Figure 2 and 4 is available in the online journal.)

density of $n_0 = 10^6 \text{ cm}^{-3}$. The initial number of electrons in this simulation is $N \approx 23n_0d^3 = 10^{32}$ electrons, which is an approximation as we only have one spatial dimension to estimate the volume from, taking this as the $FWHM = 2\sqrt{2\ln 2}d$, which is typically measured in X-ray imaging observations (e.g. Hurford et al. 2002; Kontar et al. 2008b). Here we have used a modest number of electrons, similar to that found in a small flare, or microflare (Hannah et al. 2008a,b), a typical A or B-class GOES flare. Since the rate of wave-particle interactions is proportional to electron beam density, the effects of wave-particle interaction will be present to a far greater extent in larger flares.

We approximate the background plasma density n assuming a constant of 10^{10} cm^{-3} at coronal heights, with a sharp density increase at the chromosphere level, with further steady hydrostatic increase towards the photosphere (Aschwanden et al. 2002), see Figure 1. The initial electron beam is spatially centred at $h_0 = 4 \times 10^9 \text{ cm}$, see Figures 2 and 4 for details.

The equations (2) and (3) are solved numerically using a finite difference method as described by Kontar (2001b). This is over a grid of 60 points in velocity space and 160 in position space. The fastest process here is the quasilinear relaxation, occurring on a timescale of $\tau_Q \approx n_0 n / \omega_p \sim 2 \times 10^{-5} \sqrt{n/n_0}$ seconds. Therefore we numerically solve equations (2) and (3) using a time-step at least an order of magnitude smaller. The initial spectral energy density is taken to be the thermal background which has reached a steady-state through Coulomb collisions and wave-particle emission/absorption. These simulations are ran for 1 second in simulation time, enough time for all of the electrons to reach the highest density region, lose energy and then leave the simulation grid, joining the thermal electrons.

2.1. Beam Coulomb Collisions

We start by simulating the propagation of the electron beam in the absence of waves, with only Coulomb collisions acting on the electrons, following the standard thick-target model (Brown 1971). Namely, only solving equation (2) and ignoring the first term on the right-hand side, the wave-particle interactions. The result-

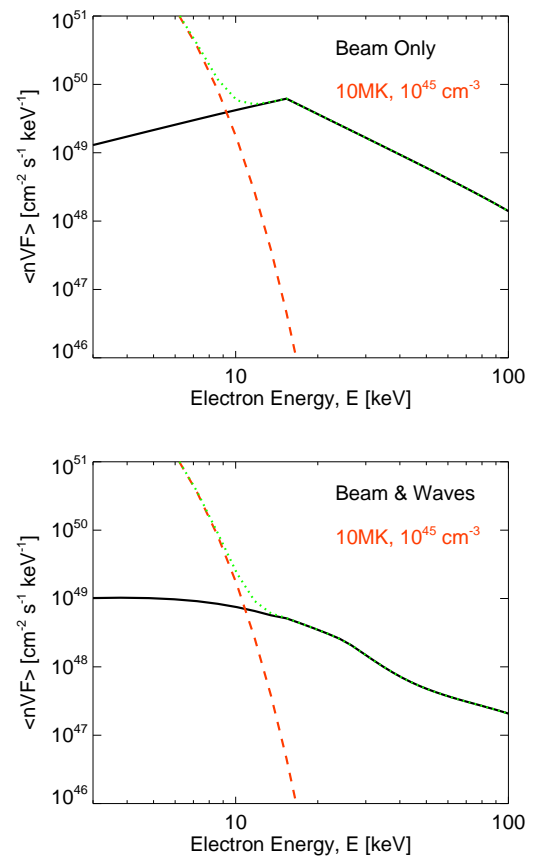


FIG. 3.— The mean electron flux spectrum $\langle nVF \rangle$ for the simulation of an electron beam with only collisional damping (top) and for the electron beam with the generation of Langmuir waves (bottom). These spatially integrated spectra are averaged over the 1sec duration of the simulations. The dashed lines are a thermal model with $T = 10 \text{ MK}$ and $EM = 10^{45} \text{ cm}^{-3}$. The dotted lines are the total spectrum.

ing electron distribution $f(v, x)$ for various times during the simulation is shown in Figure 2. The electrons with the highest velocities move quickly to lower heights where they encounter the sharply increasing background plasma density (chromosphere) below about 3 Mm. Here

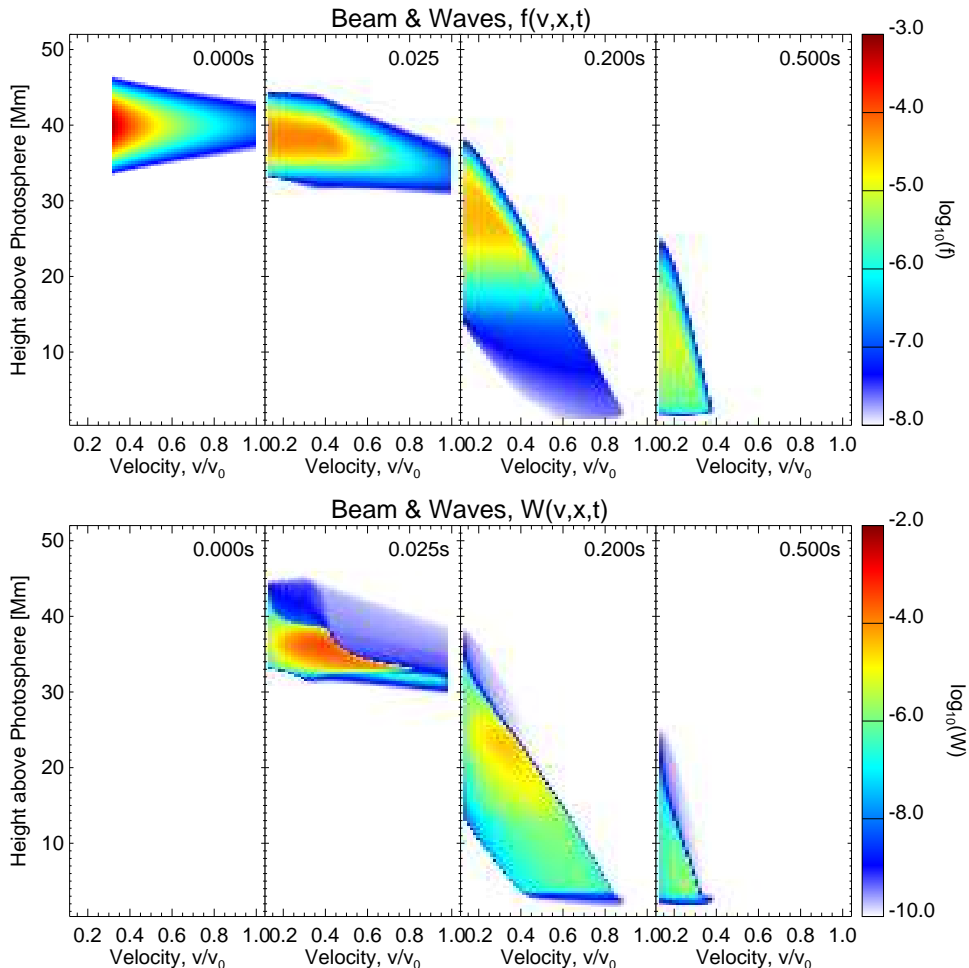


FIG. 4.— The electron distribution $f(v, x, t)$, top row, and wave spectral energy density $W(v, x, t)$, bottom row, with time increasing from left panel to right for the simulation following the progression of an electron beam including Langmuir wave response from the background plasma. W is shown against electron velocity v instead of wave number k since $k = \omega_p/v$ and to allow easy comparison between the two rows. (An animation of Figure 2 and 4 is available in the online journal.)

the Coulomb collisions quickly cause the electrons to lose energy and eventually have velocities outside of the simulation grid. At lower energies the sharp initial low energy cutoff is smoothed out through Coulomb collisions reducing the electrons velocity. The time averaged mean electron flux spectrum of purely collisional transport is shown in Figure 3. This spatially integrated mean electron flux spectrum $\langle nVF \rangle$ or $\overline{nV\overline{F}}$ is related to the simulated electron distribution $f(v, x, t)$ as $\overline{nV\overline{F}}(E, t) = A \sum [n(x)f(v, x, t)/m_e] dx$ where A is the cross-sectional area of the beam. We take this to be $FWHM^2 \approx 5.5d^2$ given our 1D simulation. The positive slope at low energies is clearly visible with the expected decreasing power-law above roughly the original low energy cutoff (Figure 3 left). Overplotted is an example model thermal spectrum to demonstrate how the local minima (dip) appears in the spectrum. A typical flare temperature of 10 MK is used, with a modest emission measure of 10^{45} cm^{-3} to match the observations of the small flare we have simulated. This is a standard thick-target spectrum, which is used to fit and interpret X-ray spectrum.

2.2. Beam-Driven Langmuir Waves

We now follow the beam propagating with Langmuir waves generated by the background plasma in response to the beam, numerically solving both equations (2) and (3). The resulting electron and spectral wave density distributions are shown in Figure 4 as a function of v and x for various times during the simulation. The electron distribution function $f(v, x, t)$ quickly flattens to form a plateau-like distribution expected for beam-plasma interaction via plasma waves (e.g. Zheleznyakov & Zaitsev 1970). The electrons together with the waves move down and eventually end up in the dense regions of the atmosphere, where the transport becomes dominated by collisions. The motion of the plasma turbulence (Figure 4) is not due to the group motion of waves, which is negligibly small $\partial\omega/\partial k = 3v_{Te}^2/v \ll v$, but appears because the Langmuir waves are locally generated and efficiently reabsorbed by the beam itself or collisionally by the surrounding plasma. The wave-particle interactions clearly changes the overall shape of spatially integrated electron flux spectrum, as shown in the right panel of Figure 3. Crucially, no positive slope is created in the non-thermal spectrum below the initial low energy cutoff, resulting in no dip in the overall model spectrum. This can be further seen when we consider the spectral index δ of the

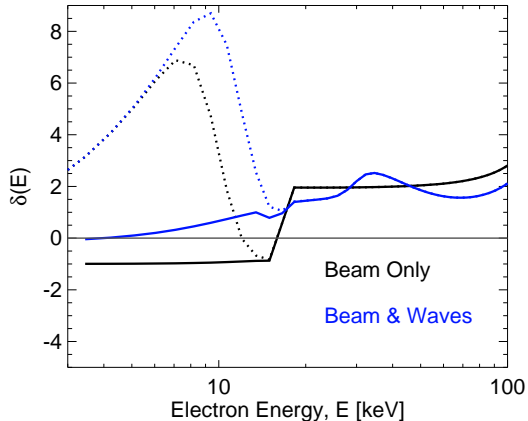


FIG. 5.— The spectral index $\delta(E) = -d \log(\langle nVF \rangle) / d \log(E)$ of the mean electron spectrum for the simulation with the electron beam only subject to Coulomb collisions (black line) and with the beam-driven Langmuir waves (blue line). The dashed line indicates the total model spectra (including thermal component) demonstrating a local minima in the beam only case.

mean electron flux spectrum as a function of energy in Figure 5. Whereas the beam only simulation produces a brief energy range where $\delta < 0$, it is always positive in the beam and wave case. The slightly reduced level of the mean electron flux spectrum also suggests that the generation of Langmuir waves leads to additional energy losses by the beam (into heating the background plasma) and higher number of energetic electrons will be required to explain the same X-ray spectra.

3. DISCUSSION & CONCLUSIONS

Considering both the temporal and spatial evolution, the mean electron flux spectrum is very sensitive to the generation of waves. The influence of wave-particle interactions is seen to flatten the spectral index of the electron spectrum $\delta(E) = d \log(\bar{nV\bar{F}}) / d \log(E)$ below the break but also up to where the beam-plasma interaction time is faster than the electron cloud time size. The artificially introduced low-energy cutoff in the injected electron spectrum disappears not only in the local electrons distribution function but also in the spatially integrated electron spectrum once wave-particle interactions is taken into account. The character of beam propagation is close to the simulation results of beam transport along open field lines, where collisions are normally ignored (Takakura & Shibahashi 1976; Magelssen & Smith 1977; Mel’Nik et al. 1999; Li et al. 2008). However, there are noticeable differences. In the simplistic treatment of spatially uniform beam, when all but quasilinear terms are ignored (e.g. Vedenov & Velikhov 1963), the generation of waves leads to an exact plateau distribution with $\delta(E) \approx 0$. Our simulations show that the spectral index, $\delta(E)$ is more than zero, which is the result of collisions. Similarly, Kontar & Reid (2009) show that the spatially integrated spectrum of particles will not deviate from an initial power-law, but only when processes leading to absorption of waves or removal of waves out of resonance are included.

The simulations in this letter are for typical microflare parameters (Hannah et al. 2008a) and given that the wave emission scales with the electron number density we would expect wave-particle interactions to have more significant, effect in large flares. Large flares could constitute multiple intermittent bursts of accelerated electrons directed along possibly different magnetic field lines. The fast time variations in hard X-ray lightcurves (Kiplinger et al. 1984) indirectly support this idea. Numerical simulations of reconnection suggest “bursty” electron acceleration (Tsiklauri & Haruki 2008) and spatially fragmented electron acceleration (Bian & Browning 2008) which could result in electron propagation along the different lines. The footpoint motion often seen in solar flares (Krucker et al. 2003) also suggest that the electrons are consecutively injected onto field lines. In this scenario an ensemble of our simulations, multiple micro-beam injections, would lead to beam densities comparable to a large flare.

The convergence of the magnetic field at chromospheric heights (e.g. Kontar et al. 2008c) has been ignored in this work, however in our simulations the overall evolution of the energetic particles in the top part of a relatively dense loop, 10^{10} cm^{-3} , is dominated by wave-particle interactions where the field is not converging. It is only in the denser chromosphere, where the field is likely to converge, that the collisions become dominant. The very fast flattening of the powerlaw distribution’s low energy cutoff by the wave-particle interactions suggests that it is unlikely that such a cutoff could develop and is therefore an unwise initial distribution for any model of coronally accelerated electrons. The non-thermal distribution flattening at low energies as it transitions into the thermal distribution seems to be a realistic model. Given how strongly the total energy in the accelerated electrons depends on a cutoff, or its behaviour at low energies approaching the thermal distribution (Emslie 2003; Galloway et al. 2005), this transition needs further study.

The work presented here is a step towards a more complete treatment of electron transport in solar flares, moving from the standard thick target model (1D velocity with collisions only) to beam-driven Langmuir turbulence (1D velocity, 1D space, collisions and wave-particle interactions). In future work we need to extend this to consider 2 or higher dimensions of velocity space, the changing magnetic field, electron scattering as well as the transition between the accelerated beam and thermal distribution.

We would like to thank the referee for their constructive comments. This work is supported by a STFC rolling grant (IGH, EPK) and STFC Advanced Fellowship (EPK). Financial support by the Royal Society grant (RG090411), The Royal Society Short Incoming Visit Grant (IV0871184), and by the European Commission through the SOLAIRE Network (MTRN-CT-2006-035484) is gratefully acknowledged.

REFERENCES

- Aschwanden, M. J., Kliem, B., Schwarz, U., Kurths, J., Dennis, B. R., & Schwartz, R. A. 1998, *ApJ*, 505, 941
- Bian, N. H., & Browning, P. K. 2008, *ApJ*, 687, L111
- Brown, J. C. 1971, *Sol. Phys.*, 18, 489
- Brown, J. C., Emslie, A. G., Holman, G. D., Johns-Krull, C. M., Kontar, E. P., Lin, R. P., Massone, A. M., & Piana, M. 2006, *ApJ*, 643, 523
- Brown, J. C., Emslie, A. G., & Kontar, E. P. 2003, *ApJ*, 595, L115
- Churaev, R. S., & Agapov, A. V. 1980, *Soviet Journal of Plasma Physics*, 6, 422
- Drummond, W. E., & Pines, D. 1964, *Annals of Physics*, 28, 478
- Emslie, A. G. 1978, *ApJ*, 224, 241
- . 2003, *ApJ*, 595, L119
- Emslie, A. G., & Smith, D. F. 1984, *ApJ*, 279, 882
- Fleishman, G. D., Stepanov, A. V., & Yurovsky, Y. F. 1994, *Sol. Phys.*, 153, 403
- Galloway, R. K., MacKinnon, A. L., Kontar, E. P., & Helander, P. 2005, *A&A*, 438, 1107
- Hamilton, R. J., & Petrosian, V. 1987, *ApJ*, 321, 721
- Hannah, I. G., Christe, S., Krucker, S., Hurford, G. J., Hudson, H. S., & Lin, R. P. 2008a, *ApJ*, 677, 704
- Hannah, I. G., Krucker, S., Hudson, H. S., Christe, S., & Lin, R. P. 2008b, *A&A*, 481, L45
- Holman, G. D. 2003, *ApJ*, 586, 606
- Holman, G. D., Sui, L., Schwartz, R. A., & Emslie, A. G. 2003, *ApJ*, 595, L97
- Hurford, G. J., et al. 2002, *Sol. Phys.*, 210, 61
- Johns, C. M., & Lin, R. P. 1992, *Sol. Phys.*, 137, 121
- Karlický, M. 2009, *ApJ*, 690, 189
- Kašparová, J., Karlický, M., Kontar, E. P., Schwartz, R. A., & Dennis, B. R. 2005, *Sol. Phys.*, 232, 63
- Kiplinger, A. L., Dennis, B. R., Frost, K. J., & Orwig, L. E. 1984, *ApJ*, 287, L105
- Klein, K.-L., Aurass, H., Soru-Escout, I., & Kalman, B. 1997, *A&A*, 320, 612
- Kontar, E. P. 2001a, *Sol. Phys.*, 202, 131
- . 2001b, *Computer Physics Communications*, 138, 222
- Kontar, E. P., Dickson, E., & Kašparová, J. 2008a, *Sol. Phys.*, 252, 139
- Kontar, E. P., Hannah, I. G., & MacKinnon, A. L. 2008b, *A&A*, 489, L57
- . 2008c, *A&A*, 489, L57
- Kontar, E. P., Piana, M., Massone, A. M., Emslie, A. G., & Brown, J. C. 2004, *Sol. Phys.*, 225, 293
- Kontar, E. P., & Reid, H. A. S. 2009, *ApJ*, 695, L140
- Krucker, S., Hurford, G. J., & Lin, R. P. 2003, *ApJ*, 595, L103
- Krucker, S., & Lin, R. P. 2008, *ApJ*, 673, 1181
- Li, B., Robinson, P. A., & Cairns, I. H. 2008, *Journal of Geophysical Research (Space Physics)*, 113, 10101
- Lifshitz, E. M., & Pitaevskii, L. P. 1981, *Physical kinetics (Course of theoretical physics, Oxford: Pergamon Press, 1981)*
- Lin, R. P., et al. 2002, *Sol. Phys.*, 210, 3
- Magelssen, G. R., & Smith, D. F. 1977, *Sol. Phys.*, 55, 211
- McClements, K. G. 1987, *A&A*, 175, 255
- Mel'Nik, V. N., Lapshin, V., & Kontar, E. 1999, *Sol. Phys.*, 184, 353
- Melrose, D. B. 1980, *Plasma astrophysics. Nonthermal processes in diffuse magnetized plasmas.* (New York: Gordon and Breach, 1980)
- Piana, M., Massone, A. M., Kontar, E. P., Emslie, A. G., Brown, J. C., & Schwartz, R. A. 2003, *ApJ*, 595, L127
- Ryutov, D. D. 1969, *Soviet Journal of Experimental and Theoretical Physics*, 30, 131
- Sui, L., Holman, G. D., & Dennis, B. R. 2007, *ApJ*, 670, 862
- Takakura, T., & Shibahashi, H. 1976, *Sol. Phys.*, 46, 323
- Tsiklauri, D., & Haruki, T. 2008, *Physics of Plasmas*, 15, 102902
- Tsyтович, V. N., & Terhaar, D. 1995, *Lectures on Non-linear Plasma Kinetics*, ed. V. N. Tsyтович & D. Terhaar
- Vedenov, A. A., & Velikhov, E. P. 1963, *Soviet Journal of Experimental and Theoretical Physics*, 16, 682
- Zheleznyakov, V. V., & Zaitsev, V. V. 1970, *Soviet Astronomy*, 14, 47
- Ziebell, L. F., Gaelzer, R., Pavan, J., & Yoon, P. H. 2008, *Plasma Physics and Controlled Fusion*, 50, 085011